Analysis of Arching Mechanism and Evolution Characteristics of Tunnel Pressure Arch

J.H. Yang [1)]***, S.R. Wang*** [2),4)]****, Y.G. Wang*** [2)] ***and C.L. Li*** [2),3)]

[1)] School of Civil Engineering and Architecture, Zhejiang University of Science and Technology, Hangzhou 310023, China.
[2)] School of Civil Engineering and Mechanics, Yanshan University, Qinhuangdao 066004, China.
[3)] Institute of Urban Construction, Hebei Normal University of Science and Technology, Qinhuangdao 066004, China.
[4)] Opening Project of Key Laboratory of Deep Mine Construction, Henan Polytechnic University, Jiaozuo 454003, China.
* Corresponding Author. E-Mail: w_sr88@163.com

ABSTRACT

Key and difficult problems are the arching mechanism and the evolution characteristics of the pressure arch in the surrounding rock after the tunnel excavation. Regarding a practical engineering as background, the definition of pressure arch of a highway tunnel was given and the boundary parameters of the pressure arch were determined by using the combination methods of theoretical analysis and numerical calculation. Considering the size of the highway tunnel excavation, the strength variation of the surrounding rock, the stress state of the highway tunnel, the geometry of the pressure arch and its mechanical evolution characteristics were revealed. Then, the engineering mechanical models were built through fitting the pressure arch centroid lines, and the mechanical stability of the pressure arch and the instability failure modes were also analyzed. The results provide a theoretical basis for the construction and reinforcing design of highway tunnels.

KEYWORDS: Highway tunnel, Surrounding rock, Pressure arch, Instability, Numerical analysis.

INTRODUCTION

In recent years, there are many failures which happened during tunnel construction as a result of the instability in the surrounding rock mass, such as working face collapse, support failure and excessive surface settlement. All of these failures will generate adverse effects on the safety and efficient construction of the tunnel engineering (Wang and Xie, 2008). It is a difficult matter to reasonably calculate the pressure in the surrounding rock and the arching mechanism along with the evolution characteristics of the pressure arch of the tunnel which were widely investigated by many practitioners and researchers.

In terms of on-site monitoring and laboratory tests, Kovari first found the existence of arch effects in loose rock in the tunnel excavation (Kovari, 1994). Then, the French engineer Fayol proposed that the rock arch could reduce the roof deformation in the chamber through the test (Müller and Fecker, 1980). In 1946, soil mechanics expert Terzaghi confirmed that the arch effect could exist in sands and put forward the existence conditions of the pressure arch (Terzaghi, 1946). In 1962, Rabcewicz proposed that the self-

Accepted for Publication on 8/10/2014.

bearing structure could form in the surrounding rock of the chamber in the New Australia Tunneling Method (NATM) (Müller and Fecker, 1980). In recent years, Lei et al. have carried out the site test for the bias pressure problem in the construction of the highway tunnel (Lei et al., 2010). Liu et al. have put forward the concept of the stress relief rate of the surrounding rock mass and completed the model test on the pressure in the rock around the tunnel (Liu et al., 2007). Li et al. have studied the mechanics behavior of the surrounding rock during the double-arch tunnel construction under the shallow condition through the physical model test (Li et al., 2012).

For the theoretical analysis and analytical calculation, Protodyakonov proposed the collapsing arch theory of the loose medium in 1907 (Bandis, 1990). In 1983, Bergman and Bjurstrom tried to design the bolt support of the chamber considering the pressure arch effect (Bergman and Bjurstrom, 1983). In 2002, the Norwegian Huang et al. proposed the identification method of the upper and lower boundaries of the pressure arch (Huang et al., 2002). Recently, the domestic scholar Wang discussed the formation and failure processes of the pressure arch in the weak surrounding rock and their interrelationships (Wang, 2007). Wang et al. conducted an analysis of the pressure arch of deep tunnel based on the elasticity theory (Wang et al., 2012). Wang and Yuan discussed the practical calculation method of pressure load of the surrounding rock of the highway tunnel through pressure arch analysis (Wang and Yuan, 2009). Li and Guo derived the load calculation formula of the deep tunnel based on the Protodyakonov's theory (Li and Guo, 2009).

In recent years, for the numerical analysis, Karakus et al. carried out finite element analysis to investigate the convergence due to the twin metro construction in the soft soil (Karakus et al., 2007). Hage and Shahrour completed the optimization analysis of the spacing and construction sequence of the double-arch tunnel by numerical simulation (Hage and Shahrour, 2008). Yu and Wang analyzed the stress state of the surrounding rock of the tunnel by finite element method and studied the pressure arch theory (Yu and Wang, 2008). Zhu et al. optimized and analyzed the construction sequence and supporting characteristics of the shallow tunnel through the three-dimensional computational model (Zhu et al., 2008) and the other related studies (Wang and Chang, 2012; Javad et al., 2013; Gazdek et al., 2014).

In summary, although some achievements on the pressure of the surrounding rock of the tunnel have been obtained by many researchers, the arching conditions, the evolution process and the instability modes of the pressure arch of the surrounding rock are still not revealed. The achievements are not forming a scientific and mature theoretical system, and more content needs to be researched further. Therefore, it is necessary to study the pressure transformation regularity, the arching conditions and the mechanics evolution characteristics of the surrounding rock of the highway tunnel based on practical engineering.

Arching Mechanism and Shape of the Tunnel Pressure Arch

Arching Mechanism of the Pressure Arch

Before a tunnel is excavated, the rock mass is in the three-dimensional stress equilibrium state. Since being removed of the restrictions, the stress in the excavation face of the tunnel changed from the three-dimensional state to the two-dimensional state after the tunnel has been excavated. With the second stress self-adjustment of the surrounding rock of the tunnel, the minimum principal stress gradually increases from zero in the free face to the original stress in the deep rock, and the maximum principal stress tends to the original stress state after experiencing the stress peak value.

As shown in Fig.1, in order to resist the non-uniform deformation of the surrounding rock of the tunnel, the stress will do self-regulating and the stress concentration area is formed in the interior of the surrounding rock, which is called the pressure arch. In general, the pressure arch exists not only in the roof of the tunnel, but also in the two sides and the floor of the tunnel. The pressure arch is one of the mechanics

characteristics of the arch structure, and it can bear the loads of its own and transfer the other loads to ensure the stability of the pressure arch.

Boundary Parameters of the Pressure Arch

In fact, around the excavated tunnel, there are different shapes of the pressure arch. In order to facilitate the study, the stress variables were defined as follows.

$$e = (\sigma_{\max} - \sigma_{\min})\sigma_{\max} \quad (1)$$

where, $\sigma_{\max}$ and $\sigma_{\min}$ are the maximum and the minimum principal stresses of the surrounding rock element after the tunnel being excavated, respectively. The principal stress of the element here is the plane stress.

As shown in Fig. 1, corresponding to the peak point A of the maximum principal stress of the surrounding rock, the boundary was defined as the inner boundary of the pressure arch. When the stress variable e was equal to 10 %, the boundary corresponding to point B was defined as the outer boundary of the pressure arch. On both lateral wall corners of the highway tunnel extending toward the depth of the surrounding rock and meeting with the inner and outer boundaries of the pressure arch along the rock rupture angle β, the closed region was the pressure arch. According to the Protodyakonov's theory and the Rankine theory, the rock rupture angle $\beta = 45° + \varphi/2$, where φ is the internal friction angle of the surrounding rock.

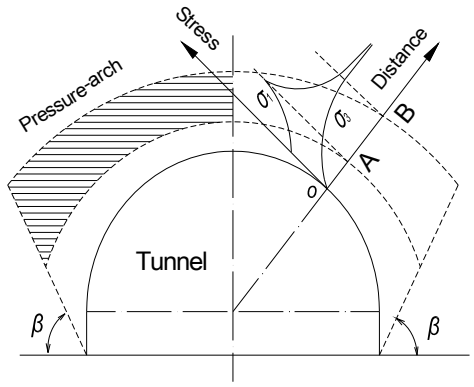

Figure (1): Boundaries of the pressure arch

The geometry of the pressure arch is shown in Fig. 2. For the sake of simplicity in the analysis, the characteristic parameters for the pressure arch were defined as such: S_1 is the vault thickness, S_2 is the waist thickness and S_3 is the skewback thickness of the pressure arch.

The mechanism of the pressure arch of the surrounding rock is as follows. When the inner boundary of the pressure arch was close to the excavation face of the tunnel, the stability of the surrounding rock was in a better state. Conversely, when the inner boundary of the pressure arch was not close to the excavation face of the tunnel, the stability of the surrounding rock was not well. The thickness of the pressure arch could indicate the degree and scope of the surrounding rock disturbed. If the thickness of the pressure arch was small, this indicated that the pressure arch could bear a small load. On the contrary, if the thickness of the pressure arch was big, the stability of the pressure arch was not well.

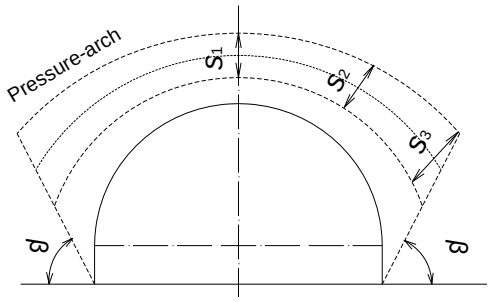

Figure (2): Geometric parameters of the pressure arch

The Tunnel and Its Computational Model

The highway tunnel section was 24 m wide and 13 m high based on practical engineering. The surrounding soil mass of the tunnel was mainly residual soil, and the stability of the tunnel was poor, meaning that the tunnel belongs to grade IV. The hydrogeological conditions were simple. According to the Code for Design of Road Tunnels in China, the physical and mechanical parameters are listed in Table 1.

As shown in Fig. 3, the three-dimension computational model was built using FLAC^{3D} technique at the depth of 80 m under the ground, and the model was in the hydrostatic stress state; namely the lateral pressure coefficient n was 1.0. The model was 80 m long, 2 m wide and 64 m high in the x-, y- and z-axis, respectively. As the tunnel could be simplified to a plane strain problem, the axial length of the tunnel was smaller. The model was divided into 10048 elements. The horizontal displacements in the x-axis and y-axis of the four lateral boundaries of the model were restricted, and its bottom in the z-axis was fixed. The vertical load was applied to the top of the model, which was equal to the weight converted from the overburden thickness. The material of the model was supposed to meet the Mohr-Coulomb strength criterion, and the physical and mechanical parameters were selected as listed in Table 1.

According to the definition of the stress variable e, after the highway tunnel being excavated, the plane stress contour and the principal stress vector distribution of the pressure arch are shown in Fig. 4.

Table 1. Physical and mechanical parameters of the surrounding rock of the tunnel

Rock classification	Density (kg/m^3)	Elasticity modulus (GPa)	Poisson ratio	Cohesion (MPa)	Friction angle (°)
Ⅳ	2200-2300	1.3-6.0	0.30-0.35	0.2-0.7	27-39
Ⅲ	2300-2500	6.0-20.0	0.25-0.30	0.7-1.5	39-50
Ⅱ	2500-2700	20.0-33.0	0.20-0.25	1.5-2.1	50-60

Analysis of the Evolution Characteristics of the Tunnel Pressure Arch

Geometric Effect Analysis of the Pressure Arch

For the convenient study, the span to height ratio k of the highway tunnel was defined as:

$$k = \frac{B}{H} \tag{2}$$

where B is the width for the tunnel section, m; and H is the height of tunnel, m.

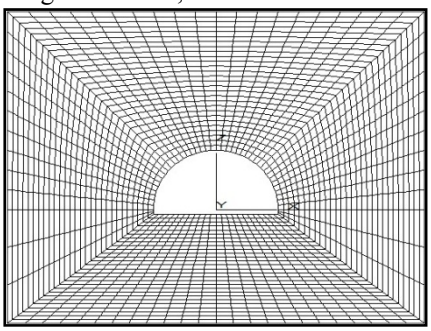

Figure (3): The computational model

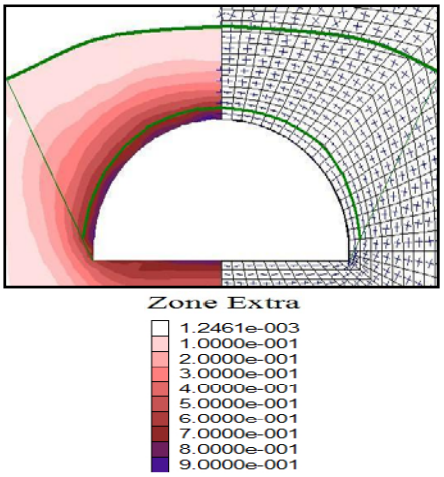

Figure (4): Boundaries and stress field of the pressure arch

Taking three sizes of highway tunnels as the study object, the span to height ratio k was 1.85, 1.64 and 1.50. The corresponding section of the highway tunnel was $B \times H$ = 24 × 13 m^2, 18 × 11 m^2 and 12× 8 m^2, respectively.

As shown in Fig.5, the shape of the pressure arch was changed from a circular arch to a flat arch, and the opening of the arches increased gradually with the increase in the span to height ratio. At the same time, the thickness of the pressure arch showed an overall increasing trend. Especially, the thickness of the foot of the pressure arch increased significantly (See Fig. 6). The results indicated that the pressure arch would bear more loads with the increase in the span-to-height ratio *k* of the tunnel.

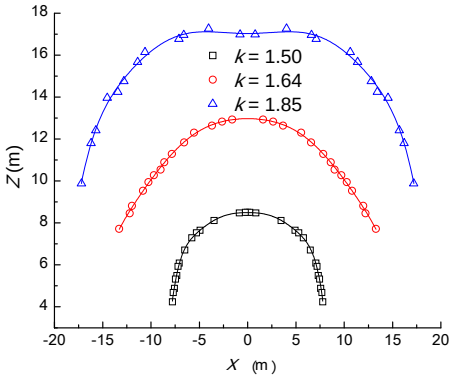

Figure (5): Pressure arch centroid line shape variation with k

Strength Effect Analysis of the Surrounding Rock

As shown in Fig.7, with the strength of the surrounding rock changing from grade IV to III to II (Table 1); namely, the strength of the surrounding rock changing from soft to hard, the height and the opening of the pressure arch gradually decreased, which showed that the pressure arch would bear less loads, and the self-stabilization of the pressure arch became better.

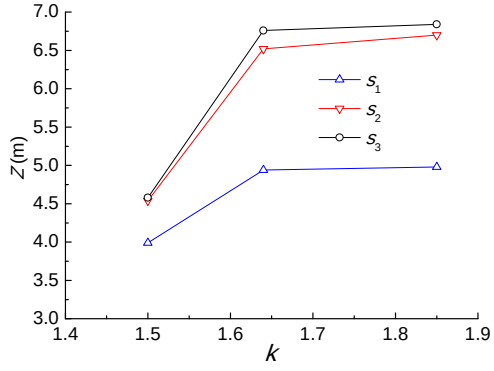

Figure (6): Pressure arch thickness variation with k

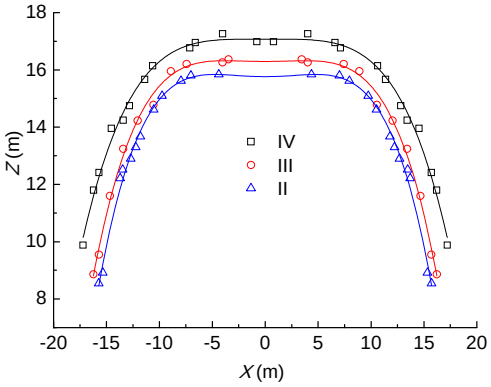

Figure (7): Pressure arch centroid line shapes with different rocks

Stress States Effect Analysis of the Pressure Arch

As shown in Fig. 8, when the lateral pressure coefficient *n* was greater than 1.0, the height of the pressure arch became bigger, and the opening of the pressure arch became smaller compared with that was 1.0. At the same time, the thickness of the vault became thicker and that of the foot of the pressure arch became thinner. (See Figs. 9 and 10).

In a contrary manner, when the lateral pressure coefficient *n* was less than 1.0, the height of the pressure arch became smaller, and the opening of the pressure arch became bigger compared with that was 1.0. (See Fig. 8). At the same time, the thickness of the vault became thinner and that of the foot of the pressure arch became thicker. (See Figs. 9 and 11).

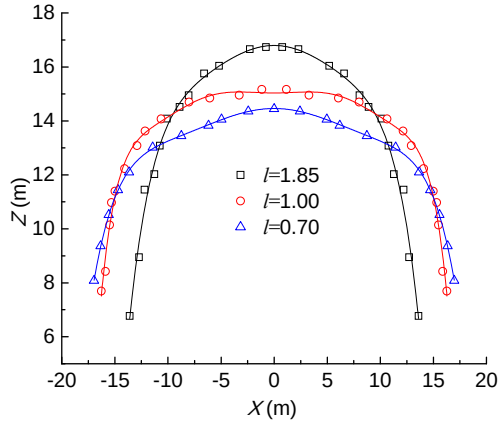

Figure (8): pressure arch centroid lines with different stress states

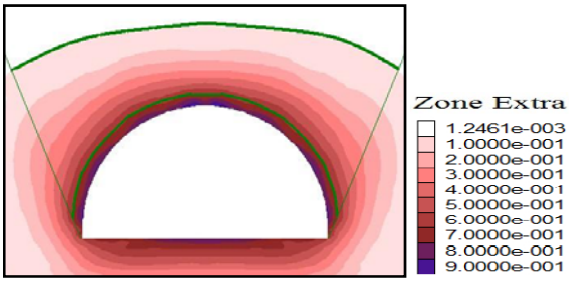

(a) Stress contour of the pressure arch

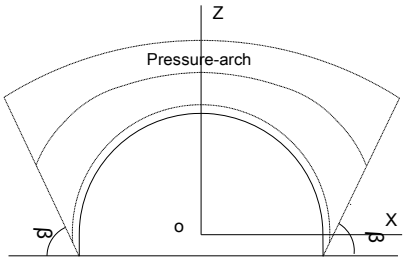

(b) Simplification of the pressure arch

Figure (9): Boundaries of the pressure arch with n = 1.00

Mechanics Stability Analysis of the Tunnel Pressure Arch

Based on the above analysis, the pressure arch structure can be simplified as in Fig. 12.

In Fig.12, there are the horizontal thrust *T*, the uniformly distributed vertical load *Q*, the uniformly distributed lateral load *nQ* and the axial compressive force *W*. For the arc CE taking the moment balance jointly to point E, the mechanics equation is:

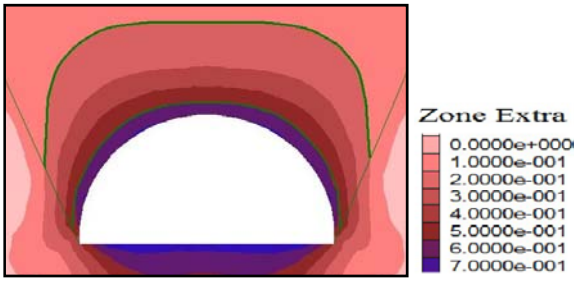

(a) Stress contour of the pressure arch

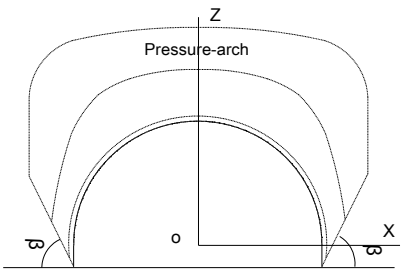

(b) Simplification of the pressure arch

Figure (10): Boundaries of the pressure arch with n = 1.85

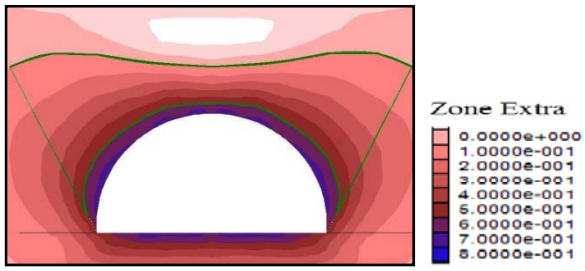

(a) Stress contour of the pressure arch

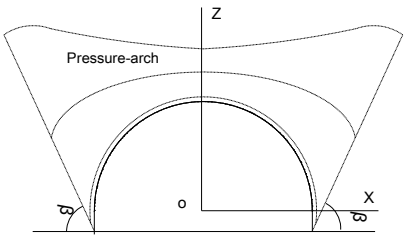

(b) Simplification of the pressure arch

Figure (11): Boundaries of the pressure arch with n = 0.70

$$\sum M_E = 0 \qquad (3)$$

$$T \times (H - z) - (Q/2) \times x^2 - (n \times Q/2) \times (H - z)^2 = 0 \qquad (4)$$

where the calculation conditions were as follows: the buried depth of the tunnel was 80 m, the excavation section of the tunnel was 24 m wide and 13 m high, the surrounding rock of the tunnel was of grade IV.

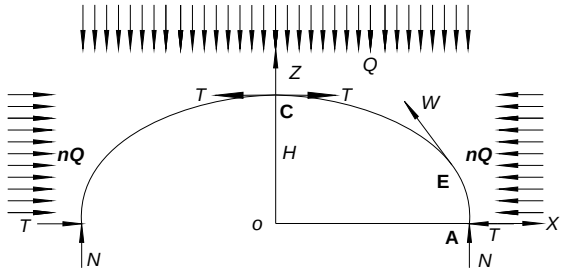

(a) The whole arch

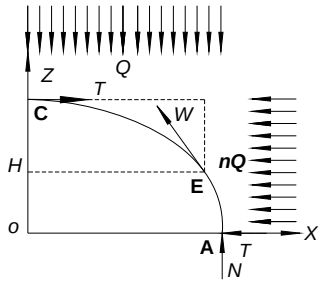

(b) Half of the arch

Figure (12): Mechanics model of the pressure arch

Supposing that the pressure arch centroid lines meet the equation $z = ax^2 + b$, then:

$$\begin{aligned} z_1 &= -0.033x^2 + 16.797 \quad (n = 1.85, -16.37 < x < 16.37) \\ z_2 &= -0.020x^2 + 15.561 \quad (n = 1.00, -18.79 < x < 18.79) \\ z_3 &= -0.019x^2 + 14.460 \quad (n = 0.70, -16.90 < x < 16.90). \end{aligned} \tag{5}$$

When equation 5 was substituted into equation 4, then:

$$T_{1\max} = 23.33Q,\ T_{2\max} = 28.53Q,\ T_{3\max} = 28.21Q \tag{6}$$

According to the Protodyakonov's pressure theory, to maintain the stability of the pressure arch, $T_{\max}$ should meet the following relationship:

$$T \le \frac{fBQ}{2} = \frac{R_c BQ}{20} \tag{7}$$

where R_c is the uniaxial compressive strength of the surrounding rock, B is the span of the pressure arch axis and f is the Protodyakonov's coefficient. In view of R_c =30 MPa for rock grade IV, which made $T_{\max}$ match equation 7, so the pressure arch curve equations z_1, z_2 and z_3 were stable.

The analytical results showed that the axial compressive force reached the maximum value at the foot of the pressure arch, so the foot of the pressure arch was liable to extrusion failure.

CONCLUSIONS

The shape of the tunnel pressure arch was changed from a circular arch to a flat arch, and the opening of the arches increased gradually with the increase in the span-to-height ratio. With the strength of the surrounding rock changing from soft to hard, the height of the pressure arch decreased gradually, which showed that the pressure arch would bear less loads, and the self-stabilization of the pressure arch became better.

When the lateral pressure coefficient was greater than 1.0, the height of the tunnel pressure arch became bigger than that of the lateral pressure coefficient of 1.0. When the lateral pressure coefficient was less than 1.0, the characteristics of the pressure arch showed the contrary manner compared with the above mentioned case. And the results showed that the feet of the pressure arch were liable to extrusion failure.

Acknowledgments

This work was financially supported by the National Natural Science Foundation of China (51474188; 51074140; 51310105020), the Natural Science Foundation of Hebei Province of China (E2014203012) and Program for Taihang Scholars. All these are gratefully acknowledged.

REFERENCES

Bandis, S.C. (1990). "Mechanical properties of rock joints". Proc. Int. Soc. Rock Mech. Symp. on Rock Joints, Rotterdam, 125-140.

Bergman, S.G., and Bjurstrom, S. (1983). "Swedish experience of rock bolting: a keynote lecture". Proceedings of the International Symposium on Rock Bolting, Rotterdam, 243-255.

Gazdek, M., Bačić, M., and Saša Kovačević, M. (2014). "Seismic quality index (SQi) of rock mass". Technical Gazette, 21 (1), 79-86.

Hage, C.F., and Shahrour, I. (2008). "Numerical analysis of the interaction between twin-tunnels: Influence of the relative position and construction procedure". Tunneling and Underground Space Technology, 23 (2), 210-214.

Huang, Z.P., Broch, E., and Lu, M. (2002). "Cavern roof stability-mechanism of arching and stabilization by rock bolting". Tunnelling and Underground Space Technology, 17 (3), 249-261.

Javad, S., Shahin, N.A., and Asad, E. (2013). "Numerical analysis of reinforced embankment over soft foundation". Journal of Engineering Science and Technology Review, 6 (3), 153-159.

Karakus, M., Ozsan, A., and Basarir, H. (2007). "Finite element analysis for the twin metro tunnel constructed in Ankara clay, Turkey". Bulletin of Engineering Geology and the Environment, 66 (1), 71-79.

Kovari, K. (1994). "Erroneous concepts behind the new austrian tunneling method". Tunnels and Tunneling, 11, 38-41.

Lei, J.S., Yang, J.S., Yang, F., and Zeng, S. (2010). "*In situ* monitoring and mechanical analysis of large-span unsymmetrical loading multi-arch tunnel". Journal of Railway Science and Engineering, 7 (4), 31-36 (in Chinese).

Li, H.B., and Guo, X.H. (2009). "Research on calculation metheods of earth pressure on muti-arch tunnel for highway". Rock and Soil Mechanics, 30 (11), 3429-3434.

Li, S.C., Yuan, C., Li, X.Z., Feng, X.D., and Li, W.T. (2012). "Model test study on mechanical behavior of extremely shallow double-arch tunnel during excavation". Journal of China Coal Society, 37 (5), 713-718 (in Chinese).

Liu, T., Shen, M.R., Gao, W.J., and Tan, D.Y. (2007). "Rock mass pressure release rate analysis for double-arch tunnel". Chinese Journal of Underground Space and Engineering, 3 (1), 50-54 (in Chinese).

Müller, L., and Fecker, F. (1980). "The elementary thought and primary principle of new Austrian tunnelling method". Underground Space, 6, 26-32.

Terzaghi, K. (1947). "Theoretical soil mechanics". John Wiley and Sons, New York.

Wang, C.B. (2007). "Study on the progressive failure mechanism of the weak crushing rock tunnel". Tongji University, Shanghai (in Chinese).

Wang, D.Y., and Yuan, J.X. (2009). "Study on the pressure calculation method of the surrounding rock of the shallow bias pressure double-arch tunnel". Chinese-Foreign Highway, 29 (2), 172-176 (in Chinese).

Wang, S.R., and Chang, M.S. (2012). "Reliability analysis of lining stability for hydraulic tunnel under internal water pressure". Disaster Advances, 5 (4), 166-170.

Wang, Y.C., Yan, X.S., Jing, H.W., Yu, L.Y., and Mou, T.A. (2012). "Study on pressure arch of deep circular tunnel". Chinese Journal of Underground Space and Engineering, 8 (5), 910-915 (in Chinese).

Wang, Y.Q., and Xie, Y.L. (2008). "The development and research of the arch tunnel in China". Highway, 8, 216-219 (in Chinese).

Yu, B., and Wang, H.J. (2008). "Pressure arch theory and the tunnel depth classification method". China Railway Press, Beijing (in Chinese).

Zhu, Z.G., Qiao, C.S., and Gao, B.B. (2008). "Analysis of construction optimization and supporting structure under load of shallow multi-arch tunnel under unsymmetrical pressure". Rock and Soil Mechanics, 29 (10), 2747-2752 (in Chinese).